Correlated Ostwald Ripening in Two Dimensions

Oleg Krichevsky and Joel Stavans
Department of Electronics, Weizmann Institute of Science, Rehovot 76100, Israel
(Received 9 November 1992)

We report results from an experimental study of coarsening in thin layers of succinonitrile in the presence of impurities. We quench the latter from the liquid phase to different temperatures within the liquid-solid coexistence region thus controlling the solid area fraction ϕ. As ϕ is increased from 0.13 to 0.40, liquidlike order develops among the coarsening crystals due to diffusional interactions. The latter give rise to local correlations between the size and rate of growth of crystals within a neighborhood of size $\xi(\phi)$. We study these and compare our findings with recent theoretical models of coarsening.

PACS numbers: 64.60.Qb, 64.70.Dv

During the late stages of a phase separation process, droplets of the minority phase undergo a coarsening process whereby small droplets shrink until they disappear while large droplets grow at their expense [1]. This coarsening process, known as Ostwald ripening, was first described theoretically within a mean-field approach by Lifshitz and Slyozov and by Wagner (LSW) [2,3] in the case of three dimensions. The LSW theory is valid in the limit of near-vanishing volume fraction ϕ of the minority phase, where droplets are widely separated and their rate of growth is determined solely by their radius and the degree of supersaturation of the majority phase. The theory predicts (1) that the average droplet radius $\bar{R}$ grows with time t as Kt^{α} with $K=\text{const}$ and $\alpha=\frac{1}{3}$ and (2) that the distribution of droplet sizes reaches a material-independent universal form when properly scaled. Numerous experiments in a variety of systems including alloys and binary liquid mixtures, as well as computer simulations and numerical calculations, have supported the qualitative character of these conclusions. However, they have revealed that both K and the droplet size distributions are functions of the volume fraction ϕ. Moreover, the measured size distributions are typically broader than the LSW prediction. It is by now well accepted that diffusional interactions [4] among droplets, which lead to interdroplet correlations, are responsible for the discrepancy between the LSW theory and experiment. Several authors have developed improved theoretical models that take into account interaction effects [5,6]. These models involve expansions in powers of the parameter $\sqrt{\phi}$, whose importance was first recognized by Tokuyama and Kawasaki [7]. To first order in $\sqrt{\phi}$, interactions give rise to two types of corrections; a direct correlation between droplet pairs whereby small droplets are likely to be surrounded by large ones, as well as a "medium polarization" in which the rate of evolution of a droplet is not only a function of its radius R but also of the droplets within a neighborhood of size $\xi(\phi)$. The models reproduce the broadening of experimental distributions while predicting that correlations do not alter the value of the LSW exponent α just as observed in experiments. Beyond measurements of the size distribution and the dependence of K on ϕ, experiments in three-dimensional systems have revealed that diffusional interactions can lead to droplet migration [8] and deformation [9]. These theoretical ideas have been extended to the two-dimensional case, where the presence of a screening length $\xi(\phi)$ is essential to avoid the divergence of the solution of the diffusion equation at infinity [10,11]. ϕ denotes in this case an area fraction. To our knowledge none of these ideas has been subjected to any experimental test.

In this paper we report results of experiments of coarsening of solid droplets surrounded by their melt in thin layers of succinonitrile. The lateral dimensions of the solid droplets are much larger than the layer thickness, and thus our system is effectively two dimensional. Our main goal was to observe correlation effects and study them for different values of the solid area fraction. Succinonitrile has the following advantages: It is transparent, the surface tension of the liquid-solid interface has very small anisotropy (~0.5%), and its melting temperature is slightly above room temperature. We used 99% pure succinonitrile purchased from Fluka. The presence of impurities is essential as they open up a liquid-solid coexistence region (43–54 °C) in which the solid area fraction can be controlled by varying the temperature, as in temperature-composition phase diagrams of binary mixtures. Two processes are involved in the evolution of the system: heat and impurity diffusion. By making the latter dominant, we insure in-plane diffusion, as heat can leak out of the system through the walls of our cells. The experiments were carried out in 25-μm-thick samples contained in cells made out of glass slides. The thermal conductivity of succinonitrile is 0.224 W/mK, which is very similar to that of the glass slides used to manufacture our cells. However, experiments carried out in cells made out of sapphire, whose conductivity is more than 10 times that of succinonitrile, yielded essentially the same results as those performed in glass-made cells, confirming that impurity diffusion is the dominant process in our system. During the coarsening process, the temperature of the samples was maintained constant with a precision of ±5 mK/h. Patterns were observed by optical micros-

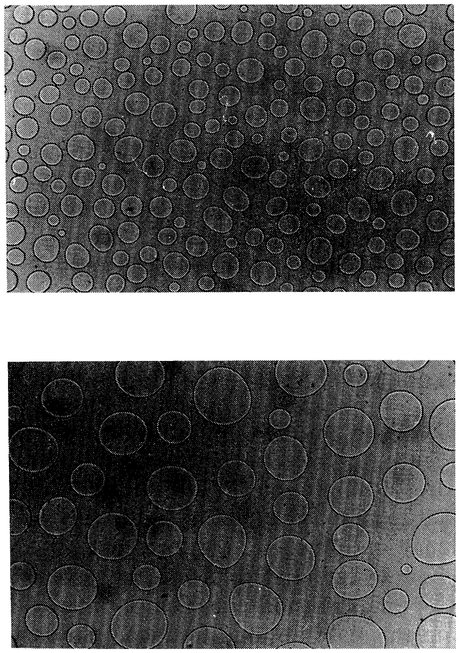

FIG. 1. Snapshots of part of the coarsening system at two different times during one of our runs with $\phi=0.40$, where the increase in the average scale and crystal deformation can be observed. The images are about 2.5 mm across.

copy and video recorded for further analysis. Initial states were produced by quenching the samples from a high-temperature liquid phase to 0 °C in order to create many nucleation sites. The temperature was then raised to desired values within the liquid-solid coexistence range to achieve different values of ϕ. During all runs, the solid area fraction was constant to within 3%. There were typically 1000 crystals of contorted shape in the field of view after a quench. In order to avoid any influence of initial conditions and due to limits in resolution, our measurements were taken when the number of crystals ranged from 300 to 30, and thus nearly a decade in the number of crystals was spanned.

Typical patterns observed during one of our runs are shown in Fig. 1. The pictures correspond to $\phi\approx0.40$. Deviations from circular shape, barely observable for $\phi=0.13$, are clearly evident in the present case. In Fig. 2 we show the measured size distribution function $f(R)$, with R given in units of $\bar{R}$ for $\phi=0.13$ and 0.40 (53 and 49 °C, respectively), together with the LSW distribution as generalized to the two-dimensional case by Rogers and Desai [12]. Each distribution comprises measurements on ten patterns recorded in the scaling regime. As ϕ increases the distributions become flatter and broader, in agreement with the behavior predicted by Marqusee [10], even though direct correlations were not included in his treatment [11]. Our measurements of the average crystal radius $\bar{R}$ as a function of time show power-law behavior with exponents in the range $\alpha=0.334\pm0.005$ for all volume fractions studied, in accordance with the theoretical predictions [10,11].

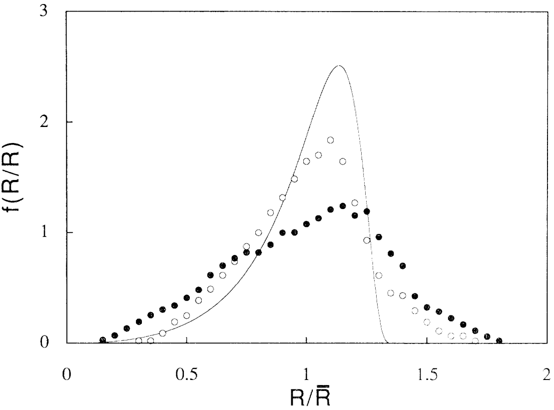

FIG. 2. Distribution of grain size $f(R)$ for $\phi=0.13$ (empty circles) and 0.40 (full circles). The solid line is the LSW generalized to the two-dimensional case by Rogers and Desai [12].

Evidence for structure induced by spatial correlations among crystals is shown in Fig. 3, where we plot the measured radial pair distribution function $g(r)$, which is proportional to the probability density of finding two crystals separated by a distance r. We show $g(r)$ for $\phi=0.13$ and 0.40, distances normalized by $\bar{R}$. In measuring $g(r)$ in each case, ten patterns well separated in time were averaged. The broad peak observed for $\phi=0.13$ gives a rough indication of the shell of nearest-neighbor crystals. For $\phi=0.40$ this peak becomes considerably more pronounced, and hence the shell of nearest neighbors becomes more well defined. This signature is reminiscent of the structure induced by repulsive interactions in ordinary fluids.

Two types of correlation effects are associated with the

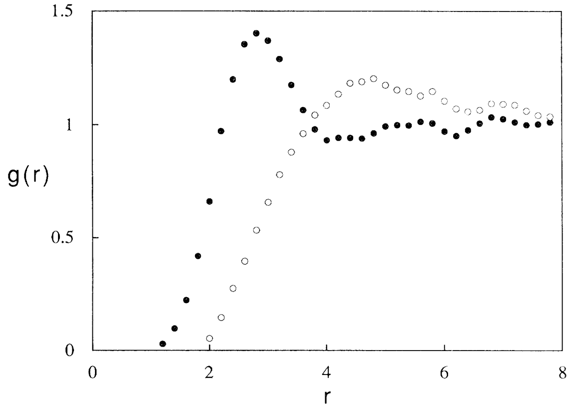

FIG. 3. Radial pair distribution function $g(r)$ for two different values of the area fraction ϕ, 0.13 (empty circles) and 0.40 (full circles), showing the evolution of gaslike behavior for low ϕ to liquidlike behavior at higher values of ϕ. Distances are given in units of the average radius $\bar{R}$.

structure described above: a direct correlation between the size of crystals and a medium polarization correlation between their rates of growth. According to the direct correlation effect small (large) crystals are more likely to be found near large (small) ones. Evidence for it was obtained by dividing all crystals into two classes L and S: those with $R > \bar{R}$ (henceforth called large) and those with $R < \bar{R}$ (henceforth called small). We then measured the probability densities $p_{s,s'}(r)$ of finding two crystals in the same class ($s = s' = L$ or S) at a distance r, and of finding them in different classes ($s = L$, $s' = S$ or $s = S$, $s' = L$). We plot these with empty and full circles, respectively, in Fig. 4 for both $\phi = 0.13$ and $\phi = 0.40$. Both probability densities have the same qualitative behavior for $\phi = 0.13$, though the probability of finding small crystals near large ones is slightly higher. The correlation is manifestly stronger for $\phi = 0.40$, where the probability of finding small crystals near large ones is strongly peaked at small distances and much larger than that of finding two nearby small or large crystals.

We turn now to medium polarization, according to which the rate of change of the size of a crystal is determined not only by its size but also by the influence of others in its surroundings. The mutual influence of the diffusion fields around two nearby crystals promotes the accelerated shrinkage of one and growth of the other, the rates of shrinkage and growth being larger than if both crystals were isolated. Thus shrinking crystals are more likely to be found in the neighborhood of growing ones and vice versa. Medium polarization is explicitly observed in our experiments when two grains with radius smaller than $\bar{R}$ happen to be sufficiently near to one another: One shrinks and the second grows at its expense, in spite of being smaller than $\bar{R}$. This growth proceeds until the first grain shrinks completely and disappears. Shrinking of the surviving grain then ensues. The effect is shown in a more general fashion making use of an appealing analogy between our problem and electrostatics used by Marder in his perturbative calculations [5]. Even though the analogy is strictly valid for small volume fractions, we still find it helpful in thinking about our system. The analogy is based on a quasistationary approximation to the diffusion equation. A charge is associated with each crystal, the charge being proportional to the rate of change of the crystal's area: $q = R\,dR/dt$. Thus shrinking (growing) crystals have negative (posi-

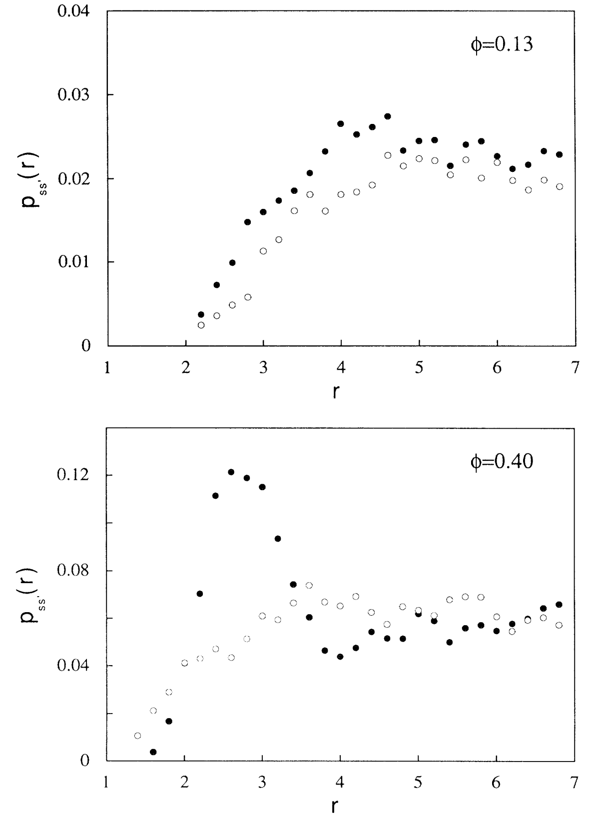

FIG. 4. Probability densities of finding two crystals both with radii smaller or larger than $\bar{R}$ at a distance r (empty circles) and of one having radius smaller and the other larger than $\bar{R}$ (full circles), for $\phi = 0.13$ and 0.40. Distances are given in units of $\bar{R}$.

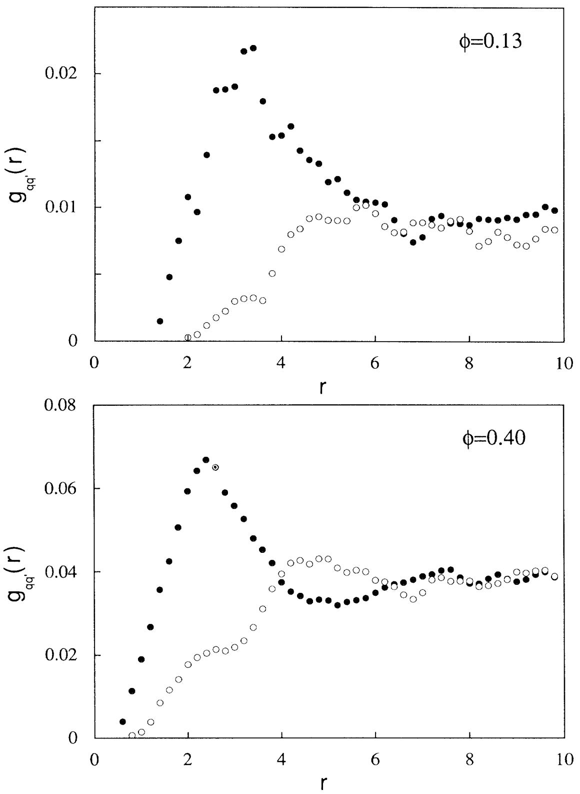

FIG. 5. Radial charge-charge correlation $g_{qq'}(r)$ as a function of distance for $\phi = 0.13$ and 0.40. Full circles: correlations of charges of opposite sign; empty circles: correlations of charges of the same sign.

tive) charge. ϕ being a constant, the total charge of the system is zero. According to the electrostatic analogy, positive and negative charges screen one another, rendering the system locally neutral. To demonstrate the existence of medium polarization in our system we measured two charge-charge spatial correlation functions $g_{qq'}(r)=\langle q(0)q'(r)\rangle$, with q' given in units of charge per unit area, one when $\mathrm{sgn}(q)=\mathrm{sgn}(q')$ and the other when $\mathrm{sgn}(q)\neq\mathrm{sgn}(q')$. Charges were measured from video frames taken at close intervals, and were assumed to be uniformly distributed along the boundary of the crystals. In Fig. 5 we show $g_{qq'}(r)$ for charges of the same sign (empty circles) and charges of opposite sign (full circles), for $\phi=0.13$ and 0.40. The correlation is much larger for short distances in the case of opposite charges, and the peak in the correlation corresponds roughly to the average nearest-neighbor distance. Opposite charges screen one another to keep the system locally neutral. The screening effect is much stronger for $\phi=0.40$ where out-of-phase oscillations in both correlations are observed for distances beyond the nearest-neighbor distance, in analogy with behavior observed in ionic liquids.

Finally, we estimate from our data the range $\xi(\phi)$ above which correlations are screened. Following Marqusee's model [10], ξ is given by

$$\xi^{-1}=2\phi\int_0^\infty R\frac{K_1(R/\xi)}{K_0(R/\xi)}f(R)dR\,,$$

where $K_1(x)$ and $K_0(x)$ are modified Bessel functions and $f(R)$ is normalized as $\int x^2 f(x)dx=1$ as prescribed by Marqusee. This formula remains unchanged if direct correlations are included [11]. Inserting our measured distributions $f(R)$ and solving numerically for ξ we find $\xi/\bar{R}=2.20\pm0.02$ for $\phi=0.40$ and $\xi/\bar{R}=0.98\pm0.01$ for $\phi=0.13$ in agreement with Marqusee's results. We point out that this formula depends weakly on $f(R)$. We also evaluated a screening length from the decay of charge with distance. The values obtained are within a factor of 2 larger than those obtained by Marqusee's prescription.

In summary, our results show that diffusional interactions in a two-dimensional system undergoing Ostwald ripening give rise to liquidlike structure among the droplets of the minority phase, and induce correlations between their sizes and rates of growth. The former are weaker than the latter. We provided explicit evidence for these correlations, estimated their range according to existing models, and found good agreement with the theoretical predictions. Structural effects, in particular, should be taken into account in any future theoretical description of large volume fraction situations. Studies of dynamical correlations, evolving shapes, pattern morphology at very high volume fractions, and ϕ-dependent rates of growth will be published elsewhere [13].

We are indebted to A. Fairhall for pattern analysis and to John Bechhoefer and E. Domany for useful discussions. One of us (J.S.) acknowledges the financial support of the Charles H. Revson and Minerva Foundations.

[1] For a review, see J. D. Gunton, M. San Miguel, and P. S. Sahni, in *Phase Transitions and Critical Phenomena*, edited by C. Domb (Academic, New York, 1983), Vol. 8, and references therein.
[2] I. M. Lifshitz and V. V. Slyozov, Zh. Eksp. Teor. Fiz. **35**, 479 (1958) [Sov. Phys. JETP **8**, 331 (1958)]; J. Phys. Chem. Solids **19**, 35 (1961); Fiz. Tverd. Tela **1**, 1401 (1960) [Sov. Phys. Solid State **1**, 1285 (1960)].
[3] C. Wagner, Z. Elektrochem. **65**, 581 (1961).
[4] J. J. Weins and J. W. Cahn, in *Sintering and Related Phenomena*, edited by G. C. Kuczynski (Plenum, London, 1973), p. 151.
[5] M. Marder, Phys. Rev. Lett. **55**, 2953 (1985); Phys. Rev. A **36**, 858 (1987).
[6] J. A. Marqusee and J. Ross, J. Chem. Phys. **80**, 536 (1984).
[7] M. Tokuyama and K. Kawasaki, Physica (Amsterdam) **123A**, 386 (1984).
[8] P. W. Voorhees and R. J. Schaefer, Acta Metall. **35**, 327 (1987).
[9] P. W. Voorhees, G. B. McFadden, R. F. Boisvert, and D. I. Meiron, Acta Metall. **36**, 207 (1988); T. Imaeda and K. Kawasaki, Physica (Amsterdam) **164A**, 335 (1990).
[10] J. A. Marqusee, J. Chem. Phys. **81**, 976 (1984).
[11] Q. Zheng and J. D. Gunton, Phys. Rev. A **39**, 4848 (1989).
[12] T. M. Rogers and R. C. Desai, Phys. Rev. B **39**, 11 956 (1989).
[13] O. Krichevsky and J. Stavans (to be published).

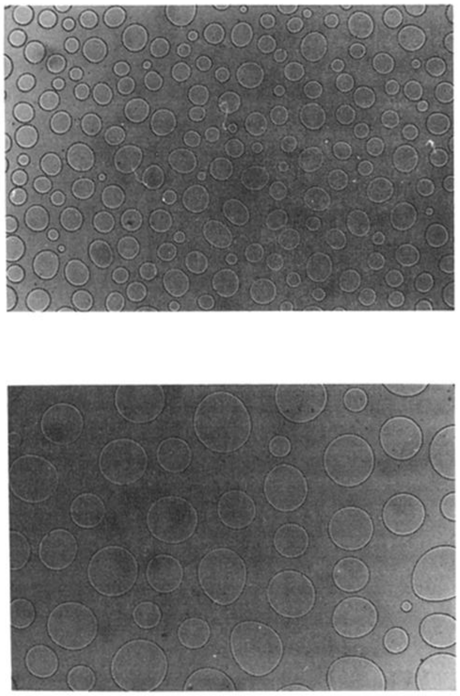

FIG. 1. Snapshots of part of the coarsening system at two different times during one of our runs with $\phi = 0.40$, where the increase in the average scale and crystal deformation can be observed. The images are about 2.5 mm across.